Low Schottky barrier height for ErSi2–x/n-Si contacts formed with a Ti cap

N. Reckinger, Xing Tang, V. Bayot, Dmitri Yarekha, Emmanuel Dubois, S. Godey, X. Wallart, G. Larrieu, A. Łaszcz, J. Ratajczak, et al.

Low Schottky barrier height for $ErSi_{2-x}/n$-Si contacts formed with a Ti cap

Cite as: J. Appl. Phys. **104**, 103523 (2008); https://doi.org/10.1063/1.3010305
Submitted: 21 August 2008 • Accepted: 17 September 2008 • Published Online: 19 November 2008

Nicolas Reckinger, Xiaohui Tang, Vincent Bayot, et al.

Low Schottky barrier height for $ErSi_{2-x}$/*n*-Si contacts formed with a Ti cap

Nicolas Reckinger,[1,a)] Xiaohui Tang,[1] Vincent Bayot,[1] Dmitri A. Yarekha,[2] Emmanuel Dubois,[2] Sylvie Godey,[2] Xavier Wallart,[2] Guilhem Larrieu,[2] Adam Łaszcz,[3] Jacek Ratajczak,[3] Pascal J. Jacques,[4] and Jean-Pierre Raskin[5]

[1]*Microelectronics Laboratory, Université catholique de Louvain, Place du Levant 3, B-1348 Louvain-la-Neuve, Belgium*

[2]*Institut d'Electronique, de Microélectronique et de Nanotechnologie, IEMN/ISEN UMR CNRS 8520, Avenue Poincaré, Cité Scientifique, 59652 Villeneuve d'Ascq Cedex, France*

[3]*Institute of Electron Technology, Al. Lotników 32/46, 02-668 Warsaw, Poland*

[4]*Laboratoire d'Ingénierie des Matériaux et des Procédés (IMAP), Université catholique de Louvain, Place Sainte Barbe 2, B-1348 Louvain-la-Neuve, Belgium*

[5]*Microwave Laboratory, Université catholique de Louvain, Place du Levant 3, B-1348 Louvain-la-Neuve, Belgium*

(Received 21 August 2008; accepted 17 September 2008; published online 19 November 2008)

In this paper, the formation of Er disilicide ($ErSi_{2-x}$) with a Ti cap on low doping *n*-type Si(100) is investigated. After deposition in ultrahigh vacuum, the solid-state reaction between Er and Si is performed *ex situ* by rapid thermal annealing between 450 and 600 °C in a forming gas ambience with a 10 nm thick Ti capping layer to protect Er from oxidation. X-ray diffraction analyses have confirmed the formation of $ErSi_{2-x}$ for all annealing temperatures. The formed films are found to be free of pinholes or pits and present a sharp and smooth interface with the Si bulk substrate. The extracted Schottky barrier height (SBH) corresponds to the state-of-the-art value of 0.28 eV if the annealing temperature is lower than or equal to 500 °C. This result demonstrates the possibility to form low SBH $ErSi_{2-x}$/*n*-Si contacts with a protective Ti cap. However, when the annealing temperature is set to a higher value, the SBH concomitantly rises. Based on our experiments, this SBH increase can be mainly related to an enhanced diffusion of oxygen through the stack during the annealing, which degrades the quality of the $ErSi_{2-x}$ film. © *2008 American Institute of Physics*. [DOI: 10.1063/1.3010305]

I. INTRODUCTION

The more the dimensions of metal-oxide-semiconductor field effect transistors (MOSFETs) are reduced toward the 10 nm node, the more the constraints on the classical implanted source/drain (S/D) tighten, due to increasing process difficulties essentially related to dopant activation to achieve (i) heavily doped junctions, (ii) extremely steep lateral profiling, and (iii) low specific contact resistance. In order to overcome these issues, it was proposed to replace highly doped S/D by metallic Schottky S/D.[1] More specifically, to reach very low specific contact resistance, it is required to work with very low Schottky barriers, ideally less than 0.1 eV.[2,3] In the case of barriers to electrons, among all existing metals, the rare-earth (RE) elements (or lanthanides) are known to present the lowest Schottky barrier height (SBH) to *n*-Si (noted as Φ_{Bn}). Only a few research groups provide a value for the SBH of RE silicides. The most studied one is Er disilicide ($ErSi_{2-x}$), which presents a SBH of about 0.28 eV if grown in ultrahigh vacuum (UHV) conditions.[4,5] In addition to exhibit the lowest Schottky barriers to electrons, RE silicides possess several other advantages such as a relatively low resistivity,[4] a low lattice mismatch with Si,[6] and the possibility of epitaxial growth.[4–6]

RE metals are also very sensitive to contamination by oxygen (during deposition and annealing) and thus quickly oxidize,[7,8] causing a deterioration of the quality of the formed silicide films and a possible increase in Φ_{Bn}.[9] This high sensitivity to oxygen implies the need to perform the annealing under special conditions. Ideally, the solid-state reaction should be performed *in situ* in UHV conditions, just after evaporation, without breaking the vacuum. In another way, if the vacuum is broken between the evaporation and the annealing, it is necessary to cover REs with a capping layer preventing the penetration of oxygen after deposition. Moreover, this layer stops the diffusion of residual oxygen during the *ex situ* annealing. The capping layer approach is interesting since it would considerably simplify the integration of RE silicides in an industrial complementary metal-oxide-semiconductor (CMOS) process. However, up to now, the efficiency of a capping layer to reach a low SBH of 0.28 eV has never been demonstrated.

A few authors investigated the formation of RE silicides with a capping layer, for instance, Pt/W/Er,[10] Pt/Si/Er,[11] Si/Er,[12] Mo/Er,[13] Pt/Er,[14] Ti/TiN/Yb,[15] or W/Er.[16] In the perspective of RE silicide integration, the question of the removal of the sacrificial protecting layer must be taken into account. In the case of Pt, aqua regia is the only known chemical mixture able to strip Pt. However, RE silicides are easily removed in a solution containing halogen ions.[17] Second, Pt was found to mix with RE metals even at 300 °C.[18] A Si capping layer is also incompatible with modern CMOS technology since the silicidation is performed all over the wafer, creating a single silicide layer that short circuits all the

a)Electronic mail: nicolas.reckinger@uclouvain.be.

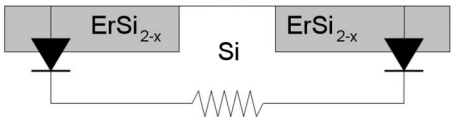

FIG. 1. Equivalent circuit of the system used to extract the SBH by an activation-energy method: two face-to-face Schottky diodes separated by a Si series resistance.

devices. W proves to be efficient to prevent oxidation but diffuses through the stack during the silicidation,[16] which could have a negative impact on the SBH. On the opposite, Ti is a good candidate to serve as capping layer, since it is readily removed in sulfuric peroxide mixture (SPM) and does not mix with REs even at 800 °C.[18] To our knowledge, no data about the SBH of RE silicides formed with a Ti cap are available in the literature. It is nevertheless worth mentioning that Liew *et al.*[19] and Yiew *et al.*[20] studied the influence of a Ti cap on the formation of $ErSi_{2-x}$ over a SiGe substrate and the formation Er germanide, respectively. However, they did not perform any SBH extraction.

To further extend the current knowledge on the properties of RE silicides, the present paper aims at investigating $ErSi_{2-x}$ thin films grown on *n*-Si(100) by *ex situ* annealing with a Ti cap. The formation of $ErSi_{2-x}$ is verified after the thermal treatment. The morphology of the formed films is studied in detail. The SBH is accurately extracted from temperature-dependent current-voltage measurements. The chemical changes in the Ti/Er/Si stack after annealing are also analyzed to examine the efficiency of the Ti capping layer as a barrier against oxygen contamination.

II. EXPERIMENTAL PROCEDURES

The starting wafers were lowly doped *n*-Si(100) bulk wafers (phosphorus-doped with a resistivity of 5–10 Ω cm). The preparation of the Si surface just before deposition is critical for the formation of high quality silicides (more specifically for RE silicides) and thus deserves a short description. The Si wafers were cleaned in SPM (50% H_2SO_4 +50% H_2O_2) for 10 min, rinsed in de-ionized water for 10 min, and dried by spinning under N_2. Then, the wafers were dipped into 1% hydrofluoric (HF) acid to remove SiO_2 grown during the SPM cleaning, rinsed, and dried as previously mentioned.

The activation-energy-based method[21] used in this paper to extract the SBH relies on specific structures consisting of two silicided contacts separated by a Si gap, as illustrated in Fig. 1. This structure simulates the source/channel/drain of a real Schottky barrier MOSFET (SB-MOSFET). The equivalent circuit of such a structure is composed of two face-to-face Schottky diodes separated by a Si series resistance (see Fig. 1). The face-to-face Schottky diodes were defined by simply fixing a mechanical mask on a Si wafer after the Si surface preparation. The use of such a mask instead of SiO_2 or Si_3N_4 allows eliminating the contribution of leakage currents arising from possible superficial reactions between the previous dielectrics and Er upon annealing.

The samples were then introduced into the evaporator immediately after the preparation steps, with the aim to limit oxide regrowth as much as possible. Then, the metal deposition was realized in an e-beam evaporator operating under UHV (base pressure $<5\times10^{-9}$ Torr). In order to clean the Er target, 25 nm of Er was sublimated just before deposition (with the blanker shut). For comparison with Ti-capped samples, we have also prepared uncapped samples.

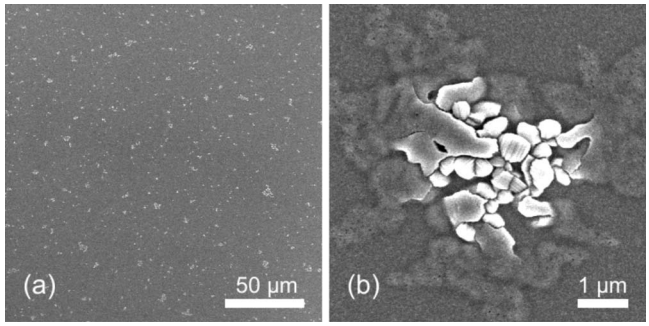

FIG. 2. (a) Low magnification SEM picture of the surface of the uncapped sample annealed for 2 min at 450 °C: the surface is scattered with many defects. (b) Focus on one of those defects.

All the samples were next heated *ex situ* by rapid thermal annealing (RTA) in forming gas (N_2:H_2 in ratio 95:5), immediately after extraction from the evaporator. The annealing was performed at 450, 500, 550, and 600 °C for 2 min, respectively. The wafers were then diced in small pieces in order to isolate the face-to-face Schottky diodes. Finally, these diodes were stuck on a ceramic chip and bonded with aluminum wires.

Formed phases were identified by θ-2θ x-ray diffraction (XRD) with the Cu $K\alpha$ radiation. The morphological characterization was performed with scanning electron microscopy (SEM) and cross-sectional transmission electron microscopy (XTEM). The electrical temperature-dependent measurements for the SBH extraction were accomplished by four-contact probing in a cryostat where the face-to-face Schottky diodes were mounted. The compositional analysis was carried out by means of depth profile x-ray photoelectron spectroscopy (XPS).

III. RESULTS AND DISCUSSION

A. Uncapped Er on *n*-Si

Figure 2(a) shows a low magnification SEM picture of the surface for the uncapped sample annealed at 450 °C. In this image, many defects of various sizes can be observed. Figure 2(b) illustrates a zoom on one of those defects. This volcanolike feature is very similar to the cracklike features in Er germanide reported by Liew *et al.*,[19] for whom the formation of those cracks could be associated to the release of stress induced by the formation of Er oxide. Typical dimensions for those volcanoes range from 0.5 to 15 μm. In the central part of the volcano, the stress was so important that the surface is completely dislocated. At the periphery, the surface visibly underwent some stress, as it appears buckled, but the stress was not high enough to break apart the layer.

Whatever the annealing temperature, the surface of the wafer is found to be nonuniformly silicided. Er is likely to oxidize when exposed to air before the annealing or/and during the annealing due to the presence of residual O_2 in the

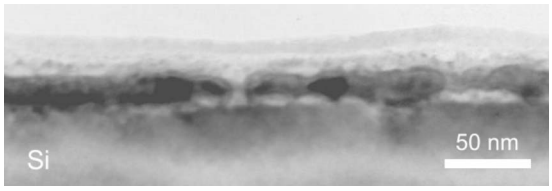

FIG. 3. XTEM micrograph for the uncapped sample annealed for 2 min at 600 °C.

RTA chamber. In Fig. 3, results of XTEM analysis performed for a silicided area of the sample annealed at 600 °C confirm that the $ErSi_{2-x}$ film is very irregular, most likely heavily oxidized.

B. Ti-capped Er on *n*-Si

The necessity of a protecting layer to prevent oxidation during annealing has been illustrated by the poor quality of $ErSi_{2-x}$ films grown without capping. In order to avoid oxidation during *ex situ* annealing, a Ti layer was deposited over Er. To identify the formed compounds and to confirm the formation of $ErSi_{2-x}$, θ-2θ XRD analyses were performed for each annealing temperature, as exhibited in Fig. 4. A very intense peak at $2\theta=27.1°$, corresponding to the (100) peak of hexagonal $ErSi_{2-x}$, was detected for all samples. The observation of such a strong peak is indicative of the formation of either highly textured or epitaxial $ErSi_{2-x}$ thin films, with an orientation relation of the type $ErSi_{2-x}(100)//Si(100)$. Another peak (at $2\theta=30.6°$) is also disclosed for all annealing temperatures. This peak neither belongs to the diffraction pattern of hexagonal $ErSi_{2-x}$ nor to the one of body-centered cubic Er sesquioxide (Er_2O_3). That peak could be relevant to a mixture phase of Er, Si, and O [Er pyrosilicate[20] or Er–Si–O (Ref. 22)]. More specifically, since Si is known to be the main diffusing species during the growth of $ErSi_{2-x}$,[23] it is likely to diffuse to the top region of the Er layer, where it is also in presence with oxygen diffusing through the Ti cap. This results in the formation of a layer containing Er, Si, and

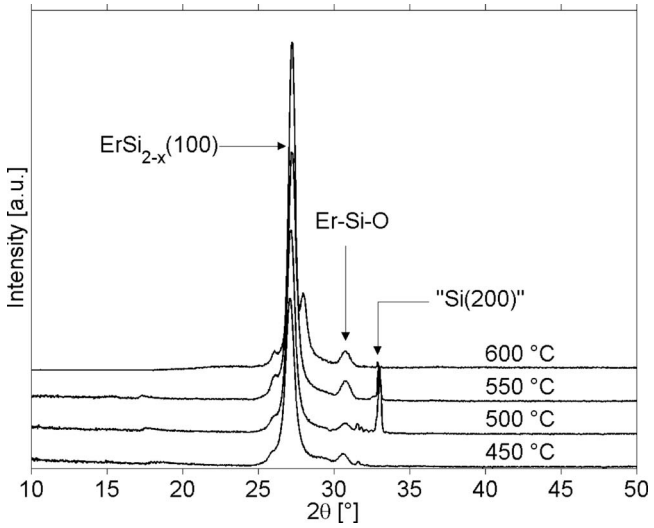

FIG. 4. XRD spectra for the Ti-capped samples annealed for 2 min at 450, 500, 550, and 600 °C, respectively. An intense $ErSi_{2-x}(100)$ peak can be observed for all annealing temperatures.

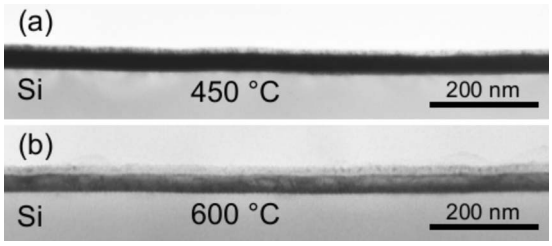

FIG. 5. Low magnification XTEM micrographs for the Ti-capped samples annealed for 2 min at (a) 450 °C and (b) 600 °C, respectively.

O above $ErSi_{2-x}$. It is worth noting that the capping layer is not detected, probably because it is amorphous or too thin. Moreover, contrary to a recent publication,[15] we have not observed the presence of diffraction peaks that could be related to Ti–Si phases.

To further investigate the transformations of the Ti/Er/Si stack upon thermal annealing, we performed XTEM analyses. Figures 5(a) and 5(b) exhibit low magnification XTEM micrographs of samples annealed by RTA at 450 and 600 °C, respectively (without cap stripping). These images provide information on the global morphology of the $ErSi_{2-x}$ films. The $ErSi_{2-x}/Si$ interface is found to be remarkably sharp in both cases. This result agrees with Chen *et al.*,[24] showing that RTA eliminates interface roughness often observed for Er silicides formed in furnace. Besides, the capping layer remains intact and is visibly not mixed with Er during the annealing. No pit or pinhole was observed in the $ErSi_{2-x}$ film, which could be due to the presence of the capping layer. Recently, Huang *et al.*[16] indeed showed that capping layers can improve the morphology of $ErSi_{2-x}$ thin films.

In order to depict the quality of the deposition, we display in Fig. 6(a) a high magnification micrograph for the as-deposited Ti/Er/Si stack. The Er and Ti thicknesses measured from Fig. 6(a) are found to be close to their respective initial target of 25 and 10 nm. It is also interesting to notice the presence of a thin Er–Si amorphous layer between the Er layer and the Si substrate. Such an intermixing of two metallic elements to form amorphous interlayers is called solid-

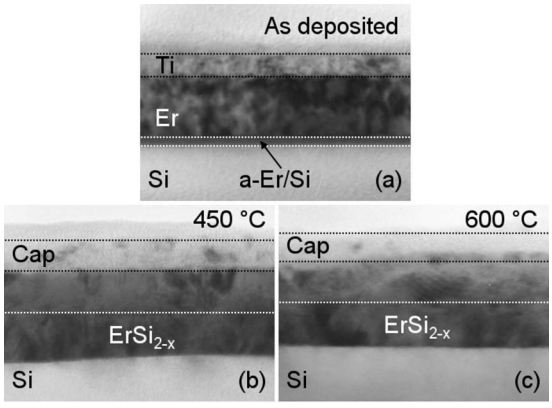

FIG. 6. High magnification XTEM micrographs of Ti-capped samples (a) before annealing, (b) after annealling for 2 min at 450 °C, and (c) after annealing for 2 min at 600 °C.

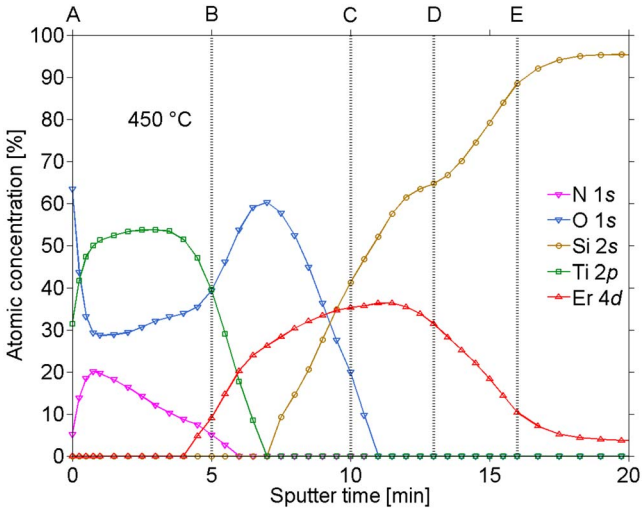

FIG. 7. (Color online) XPS atomic concentration depth profile of the Ti-capped sample annealed for 2 min at 450 °C. The markers A to E indicate specific positions along the profile.

state amorphization.[25] In a previous report,[13] it was already mentioned to occur after the deposition of Er over Si, without any annealing.

Figures 6(b) and 6(c) present higher magnification micrographs for the samples annealed at 450 and 600 °C, respectively. From these figures, it clearly appears that the stacks resulting from annealing at 450 and 600 °C are divided into three distinct layers: the capping layer on the top, an intermediate layer of unknown composition, and finally the $ErSi_{2-x}$ one. Even though the exact composition of the intermediate layer is not known, it is likely mainly composed of Er atoms since the capping layer and the Er layer do not mix. It probably corresponds to the XRD peak identified as Er–Si–O. However, for 600 °C, it turns out that the intermediate layer thickens to the detriment of the $ErSi_{2-x}$ layer.

XRD and XTEM analyses have allowed to evidence that the Ti/Er/Si stack has been transformed into three distinct layers after annealing: (i) the capping layer mainly containing Ti, (ii) the intermediate layer possibly consisting of an Er–Si–O alloy, and (iii) the bottom one composed of $ErSi_{2-x}$. In order to reveal the nature of the second layer and to investigate the modifications of the chemical composition in the stack after thermal treatment, XPS depth profiling has been performed. Core level spectra were recorded from nitrogen (N 1*s*), titanium (Ti 2*p*), oxygen (O 1*s*), erbium (Er 4*d*), and silicon (Si 2*s*). The depth profile analysis was achieved by sputtering using an Ar^+ ion gun operated at 2 keV with a beam raster of 2×2 mm^2. Figure 7 exhibits the atomic concentration depth profile of the Ti/Er/Si stack annealed at 450 °C. Figure 8 displays the corresponding core level spectra for N 1*s*, Ti 2*p*, O 1*s*, Er 4*d*, and Si 2*s*, respectively. For each element, we have limited the plot to their zone of interest. To facilitate the discussion, we have used different markers to locate specific positions in Figs. 7 and 8.

The Ti 2*p* signal can be found down to a depth corresponding to 7 min of sputter time. The top surface of the capping layer (marker A) is essentially composed of Ti dioxide (TiO_2), as indicated by the binding energies of the Ti $2p_{3/2}$ (458.4 eV) and O 1*s* (530.1 eV) peaks.[26] A small nitrogen amount (about 5% in atomic concentration) is also present at this place. The corresponding N 1*s* peak of 397.1 eV is relevant to TiN_x.[27] Just below the surface, at a sputter time of 0.5 min, the Ti $2p_{3/2}$ peak is shifted to a binding energy of 455.3 eV, while the O 1*s* peak is shifted to 531.4 eV, revealing a strong change in chemical composition. Indeed, an O 1*s* peak of 531.4 eV is no more relevant to TiO_2 but rather to the TiO suboxide.[28]

Within the subsurface region of the capping layer [between 0.5 and 5 min (marker B)], the characteristic binding energy of N 1*s* shifts from 397.1 to 397.8 eV, indicative of a progressive decrease in the N concentration in a TiN_x alloy,[27] as also confirmed by the progressively decreasing atomic concentration. Simultaneously, the Ti $2p_{3/2}$ binding energies are comprised between 455.3 eV (0.5 min) and 454.7 eV (5 min). The peak of O 1*s* remains centered around 531.7 eV. It results that the capping layer after annealing can be characterized by a TiO_xN_y composition. The Ti concentration is almost constant, while the oxygen and nitrogen concentrations are, respectively, increasing and decreasing with depth. It is worth noting here that nitrogen was only found in the capping layer.

At 5 min (marker B), the presence of Er is detected with a peak of 170 eV, while the peak of oxygen is shifted to 531.3 eV. Both these binding energies correspond to Er oxide (ErO_x).[29] The sputter time of 5 min clearly marks the frontier between the Ti cap and the Er layer. The occurrence of Ti at the surface of the Er layer is likely due to some Ti redeposition after sputtering.

The layer comprised between 5 and 7 min is mainly composed of ErO_x. In that layer, oxygen is indeed characterized by a peak of 531.3 eV. From 7.5 min, the presence of Si is detected with a binding energy characteristic of $ErSi_{2-x}$ (150.4 eV). The Er 4*d* peak progressively shifts from 169.6 (8 min) to 168.4 eV (10 min), toward the typical peak of $ErSi_{2-x}$,[29] indicating that the proportion of $ErSi_{2-x}$ increases comparatively to ErO_x. The layer comprised between 5 and 10 min (marker C) of sputtering time is thus a mixture of ErO_x and $ErSi_{2-x}$ with a progressively decreasing amount of ErO_x. That layer likely corresponds to the intermediate layer observed by XTEM and revealed by the peak at $2\theta=30.6°$ in the XRD data. The previous results indicate that it seems to be composed of a mixture of Er, Si, and O.

We can consider that the $ErSi_{2-x}$ layer, properly speaking, begins at 10 min of sputtering time (marker C). A small amount of oxygen is found at the top of the silicided film. From 11 min of sputtering time, the oxygen signal escapes detection. The layer between 11 and 13 min (marker D) is composed of pure $ErSi_{2-x}$ (with Er 4*d* and Si 2*s* peaks of 167.8 and 150.4 eV, respectively). At 13.5 min, the Si 2*s* binding energy starts to progressively shift to the peak of elemental Si (151 eV), meaning that the Si bulk is close to that position. The characteristic energy of elemental Si is registered after 16 min (marker E). It is worth noting here that, even if Er appears in the depth profile after 13 min, there is no more $ErSi_{2-x}$ since the Si 2*s* peak begins to shift

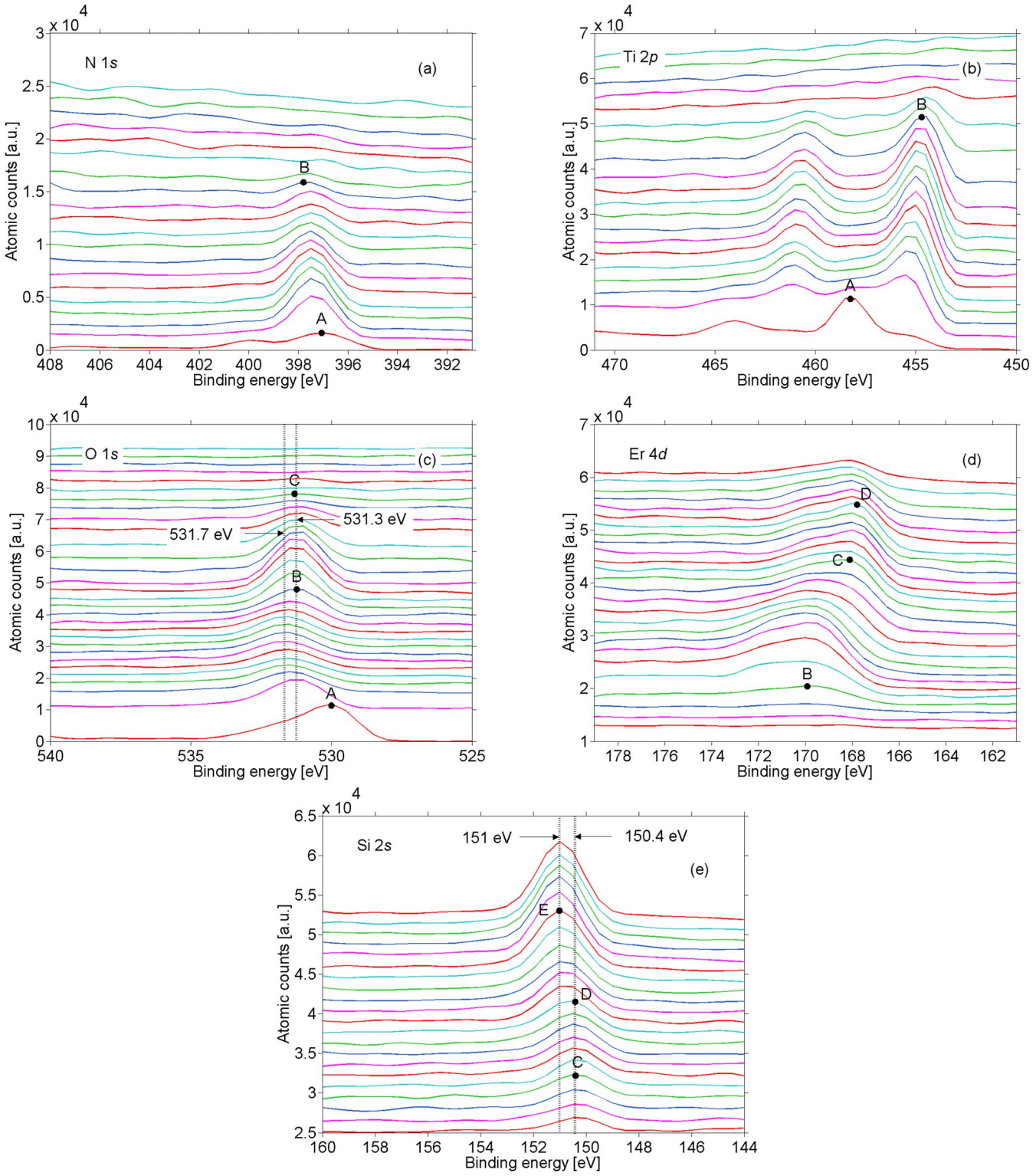

FIG. 8. (Color online) Series of spectra for the Ti-capped sample annealed for 2 min at 450 °C corresponding to the emission lines of (a) N 1*s*, (b) Ti 2*p*, (c) O 1*s*, (d) Er 4*d*, and (e) Si 2*s*, respectively.

to 151 eV. Once again, we believe that some Er is redeposited and even buried into the Si substrate during the sputtering process.

It is worth commenting here that it is in fact relatively difficult to precisely determine by XPS where the frontier between the intermediate layer and the $ErSi_{2-x}$ layer is located, since there might be some Er redeposition on the substrate during the sputtering procedure. XTEM is a more appropriate tool for that purpose. It appears nonetheless clear that there is succession of three layers of different compositions, but their respective location in the XPS profile must be considered as approximative. This illustrates the necessity of correlating the results of different complementary investigation methods such as XTEM, XRD, and XPS to get a good

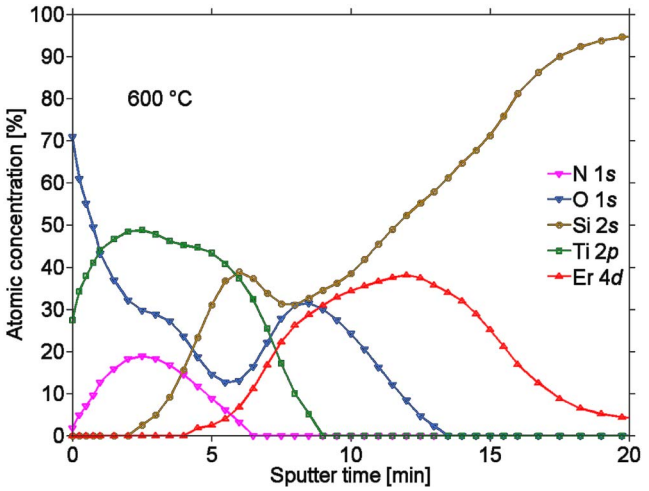

FIG. 9. (Color online) XPS atomic concentration depth profile of the Ti-capped sample annealed for 2 min at 600 °C.

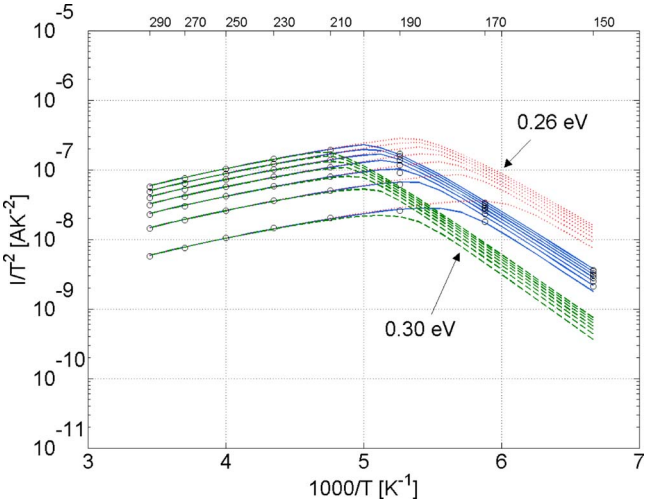

FIG. 10. (Color online) Experimental Arrhenius plot (circles) extracted from I-V_{4c}-T characteristics and the corresponding fit (solid curves), for the Ti-capped sample annealed for 2 min at 450 °C. The selected voltages range from 0.1 to 1 V by steps of 0.15 V for measurement temperatures ranging from 290 down to 150 K by steps of 20 K. The extracted SBH is equal to 0.28 eV. A small increase (dashed curves for Φ_{Bn}=0.30 eV) or decrease (dotted curves for Φ_{Bn}=0.26 eV) in Φ_{Bn} results in a down or upshift of the theoretical curves comparatively to the reference curve.

overall picture of the transformations that the stack has undergone during the heating.

Figure 9 exposes the atomic concentration depth profile of the Ti/Er/Si stack annealed at 600 °C. A very similar analysis can be made for this sample, except for a few clear differences. First, we have found out that oxygen penetrates deeper into the stack, which is understandable since the annealing temperature is substantially higher. It is also striking to observe that Si has diffused appreciably closer toward the surface. In consequence, contrary to Fig. 7, we can see the simultaneous occurrence of Ti and Si in the last layers of the cap, which could be a sign of the formation of Ti–Si phases. However, it is known that the binding energies of Ti and Si remain nearly unaffected by alloying in $TiSi_2$,[26] which is not the case here. Another consequence of the enhanced Si diffusion is that the $ErSi_{2-x}$ and ErO_x layers are less distinctly separated and interpenetrate each other, as already disclosed by the XTEM results. Indeed, the presence of $ErSi_{2-x}$ extends on a more important part of the stack, between 5 and 13 min, as testified by the Si 2*s* peak of 150.4 eV. In addition, the presence of a pure $ErSi_{2-x}$ layer (without apparent oxygen contamination), restricted to the region comprised between 11 and 13 min, can be identified. After 16 min of sputtering, the Si bulk is reached.

The SBH extraction was performed using I-V measurements at temperatures ranging from 290 to 150 K with a step of 20 K. Current versus voltage curves of face-to-face Schottky diodes were obtained by four-contact measurements. A voltage (V_{2c}) was applied between two contacts and the real voltage drop (V_{4c}) is measured between the two other ones. The experimental I-V_{4c}-T curves are then transformed into an Arrhenius plot (I/T^2 versus $1/T$) for some selected biases. The Arrhenius plot is fitted thereafter with a complete Schottky transport model that continuously combines thermionic emission (TE), field emission, and barrier lowering (BL) due to image charge. An identical measurement procedure has been accomplished for the samples annealed at 450, 500, 550, and 600 °C, respectively. Figure 10 presents the experimental Arrhenius plot (circles) extracted from I-V_{4c}-T characteristics and the corresponding fit (solid curves), for the sample annealed at 450 °C. The selected biases were 0.1 up to 1 V by step of 0.15 V. The extracted barrier is found to be equal to 0.28 eV, identical to the smallest SBH found in literature for $ErSi_{2-x}$.[4,5] It is also worth noting that experimental and theoretical data fit remarkably well. Furthermore, a small increase (dashed curves for Φ_{Bn} =0.30 eV, in Fig. 10) or decrease (dotted curves for Φ_{Bn} =0.26 eV, in Fig. 10) in the SBH in the model results in a clearly visible down or upshift of the theoretical curves comparatively to the reference curve corresponding to 0.28 eV. This indicates the high sensitivity of the model that allows a very accurate determination of the SBH. Moreover, the model allows an accurate fit on the whole measurement temperature range, suggesting a low level of interfacial contamination. Indeed, it was recently pointed out that deviations from the TE model for $ErSi_{2-x}$ Schottky diodes are caused either by SBH inhomogeneities[30] or trap-assisted tunneling,[31] both most likely due to some interfacial contamination. Since we do not observe such deviations from the TFE+BL model, the contamination level should be very low for our samples.

The presence of a small oxygen concentration at the interface was previously shown to be responsible for SBH augmentation.[9] In consequence, the state-of-the-art SBH of 0.28 eV manifests the efficiency of the Ti capping to preserve the $ErSi_{2-x}$/Si interface from oxygen diffusing through the cap during the thermal treatment. Another possible source of contamination in oxygen is related to the degree of cleanness of the Si surface prior to evaporation, more specifically the presence of a very thin layer of Si oxide. It is known that the presence of such a thin interfacial oxide before evaporation causes a dramatic increase in the SBH after heating.[32] For that reason, possible oxide regrowth in ambient air before the introduction in the evaporation chamber should be very limited in the present case. Consequently, the

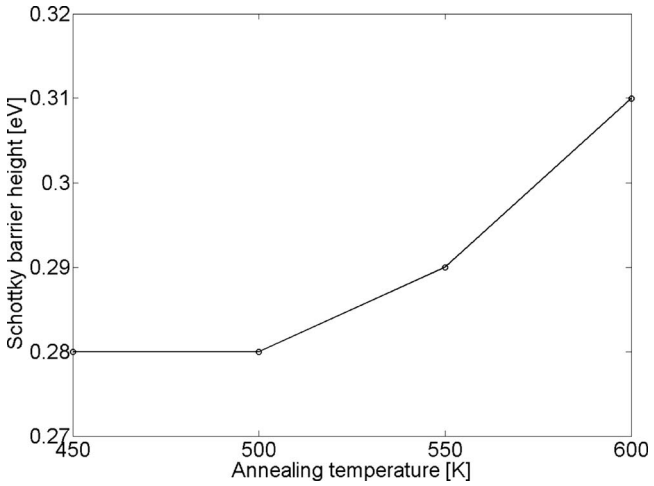

FIG. 11. SBH versus the annealing temperature.

simple cleaning method (SPM+HF dip) used here appears sufficient to reach a low SBH, without the need of a complicated *in situ* procedure to prepare the Si surface.[33] Finally, the low SBH also indicates that, contrary to W,[16] Ti does not diffuse to the $ErSi_{2-x}$/Si interface since the presence of interfacial Ti silicide would likely be responsible for a SBH augmentation owing to the high SBH of Ti silicide (around 0.6 eV). This confirms that Er and Ti do not intermix during the silicidation.[18]

Figure 11 summarizes the SBH for all annealing temperatures. It can be observed that there is a plateau at 0.28 eV for the two lowest annealing temperatures (450 and 500 °C). However, as and when the annealing temperature is increased, the SBH is slightly increased as well and amounts to 0.31 eV at 600 °C. Very few research groups have proposed hypotheses to account for the SBH increase comparatively to the state of the art of 0.28 eV. Unewisse and Storey[5] identified a correlation between the SBH and the degree of roughness of the $ErSi_{2-x}$/Si interface. Alternatively, Muret *et al.*[9] proposed that the oxygen concentration in $ErSi_{2-x}$ is directly related to the SBH: the higher the concentration, the higher the SBH.

Since the XTEM investigation did not exhibit any significant variation between the interfaces of samples heated at 450 and 600 °C (the interface was smooth in both cases), we suspect that oxygen contamination might play a role in the SBH increase. To verify this hypothesis, the photoemission measurements of the Er 4*d* core levels have been fitted with a standard linear least-squares deconvolution procedure. Such a procedure allows separating the respective contributions of ErO_x and $ErSi_{2-x}$ in the Er 4*d* profile and thereby determining which compound is preponderant at the interface. The $ErSi_{2-x}$/Si interface can be determined from the Si 2*s* core level spectra, as the depth in the stack where the Si 2*s* peak starts to shift from the peak relevant to $ErSi_{2-x}$ (150.4 eV) to the peak relevant to elemental Si (151 eV). Figures 12(a) and 12(b) show the resulting decomposition of the Er 4*d* profile into its Er 4*d* (ErO_x) and Er 4*d* ($ErSi_{2-x}$) components, for 450 and 600 °C, respectively. Figure 12(c) illustrates the extracted basis spectra used for the deconvolution: the peak at 167.8 eV is relevant to $ErSi_{2-x}$ while the peak at 169.8 eV is relevant to ErO_x. By integrating the surface under the profile curves exhibited in Figs. 12(a) and 12(b), we have calculated the Er 4*d* (ErO_x) proportion of the total Er 4*d* profile for each temperature.

First, we have found out that no interfacial oxygen is recorded at 600 °C, within the experimental accuracy. However, when we have compared the progression of the oxidation front [defined as the maximum of the ErO_x component, as illustrated in Figs. 12(a) and 12(b)] in the direction of the interface at 450 and 600 °C, we have discovered that it has got appreciably closer to the interface for 600 °C. Moreover, the proportion of ErO_x has increased from 28% to 36% between 450 and 600 °C. These two observations show that the $ErSi_{2-x}$ film grown at 600 °C is more contaminated by oxygen because the capability of the Ti cap to prevent oxygen diffusion during the silicidation is reduced at higher annealing temperature. Even though no interfacial oxygen can be detected by XPS (with a 0.1–0.5 at. % detection limit), we cannot exclude the occurrence of a very small oxygen concentration that could result in a slight SBH augmentation, as already mentioned here above. Alternatively, this enhanced diffusion could provoke a slight morphological degradation of the $ErSi_{2-x}$/Si interface, which could in turn affect the SBH.[5] Based on the XTEM micrographs presented here, we cannot totally revoke the roughness argument to explain the SBH increase. Planview high resolution TEM would provide more information. However that may be, the SBH extraction based on face-to-face Schottky diodes (and in consequence, the SBH itself) proves to be remarkably sensitive to the intrinsic characteristics of the metal-semiconductor interface.

IV. CONCLUSION

In summary, this paper has presented a detailed study of Er-based silicides thermally activated by RTA with a Ti protecting layer between 450 and 600 °C. Morphological and electrical characterizations have served as complementary analysis tools, consolidating each other in the interpretation of the experimental results. The XRD investigation has highlighted the formation of $ErSi_{2-x}$ for all annealing temperatures, together with the systematic occurrence of an unknown weak peak. TEM analyses have shown that the grown $ErSi_{2-x}$ films exhibit a smooth and flat interface. Moreover, no pinholes or pits have been discovered in the $ErSi_{2-x}$ film. XPS investigations have enabled us to determine that the unidentified peak can be related to an Er–Si–O ternary compound. It was also shown that the Ti cap does not mix with Er during the heating. The extracted SBH amounts to 0.28 eV if the annealing temperature is lower than or equal to 500 °C, identical to the lowest Φ_{Bn} ever reported in the literature for low doping *n*-Si substrates. This fact illustrates that a Ti cap can efficiently preserve the interface from contamination. However, if the annealing is performed at 600 °C, the SBH is found to increase to 0.31 eV. XPS analyses have shown that the interface with Si is apparently free of oxygen at 600 °C. Still, the comparison of the deconvolution results of the Er 4*d* XPS profile to its Er 4*d* (ErO_x) and Er 4*d* ($ErSi_{2-x}$) components between 450 and 600 °C has illus-

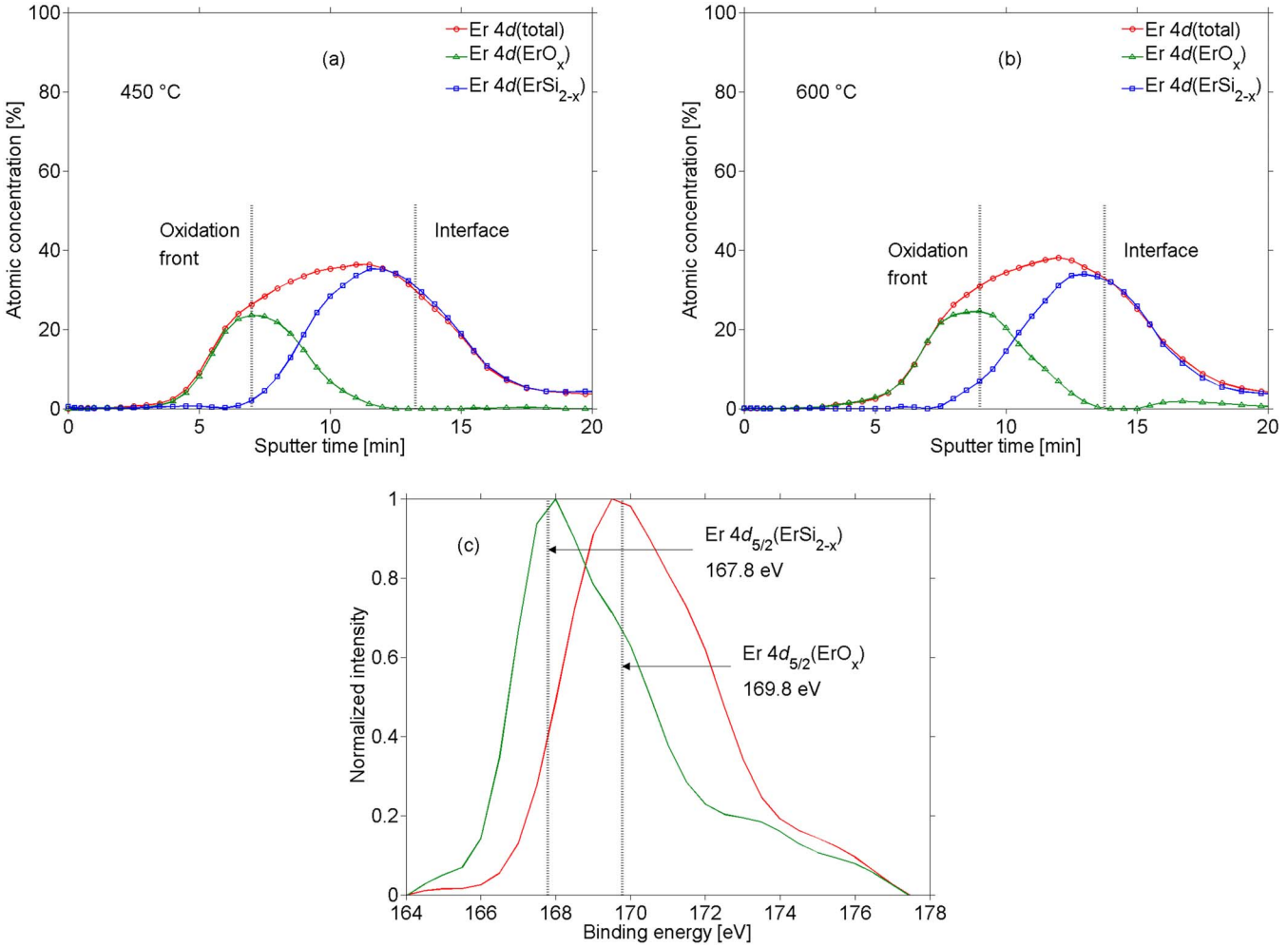

FIG. 12. (Color online) Deconvolution of the Er 4*d* atomic concentration depth profile for the Ti-capped samples annealed for 2 min at (a) 450 °C and (b) 600 °C, respectively. (c) Extracted basis spectra used for the deconvolution: 167.8 and 169.8 eV are binding energies relevant to $ErSi_{2-x}$ and ErO_x, respectively.

trated that the oxygen diffusion is more elevated at 600 °C. The proportion of ErO_x in the Er 4*d* profile is consequently found to be higher. This difference can be attributed to the limited impermeability of the thin Ti capping layer to oxygen when the annealing temperature is too high. Even though we have not found direct evidence to account for the SBH increase, many experimental facts designate the enhanced oxygen penetration as responsible for it, via slight interfacial oxygen contamination and/or roughness.

ACKNOWLEDGMENTS

This work was supported by the European Commission through the METAMOS project (METAllic S/D architecture for advanced MOS technology-STREP-016677). The authors would like to thank P. Simon, M. Zitout, D. Spôte, N. Mahieu, B. Katschmarskyj, A. Crahay, and C. Renaux for their assistance during the fabrication and the measurements.

[1]J. M. Larson and J. P. Snyder, IEEE Trans. Electron Devices **53**, 1048 (2006).
[2]D. Connelly, C. Faulkner, and D. E. Grupp, IEEE Trans. Electron Devices **50**, 1340 (2003).
[3]D. Connelly, C. Faulkner, and D. E. Grupp, IEEE Electron Device Lett. **24**, 411 (2003).
[4]J. Y. Duboz, P. A. Badoz, F. Arnaud d'Avitaya, and J. A. Chroboczek, Appl. Phys. Lett. **55**, 84 (1989).
[5]M. H. Unewisse and J. W. V. Storey, J. Appl. Phys. **73**, 3873 (1993).
[6]J. A. Knapp and S. T. Picraux, Appl. Phys. Lett. **48**, 466 (1986).
[7]J. E. Baglin, F. M. d'Heurle, and C. S. Petersson, Appl. Phys. Lett. **36**, 594 (1980).
[8]R. D. Thompson, B. Y. Tsaur, and K. N. Tu, Appl. Phys. Lett. **38**, 535 (1981).
[9]P. Muret, T. A. Nguyen Tan, N. Frangis, and J. Van Landuyt, Phys. Rev. B **56**, 9286 (1997).
[10]K. N. Tu, R. D. Thompson, and B. Y. Tsaur, Appl. Phys. Lett. **38**, 626 (1981).
[11]P. L. Janega, J. McCaffrey, and D. Landheer, Appl. Phys. Lett. **55**, 1415 (1989).
[12]C. H. Luo, G. H. Shen, and L. J. Chen, Appl. Surf. Sci. **113–114**, 457 (1997).
[13]C. H. Luo and L. J. Chen, J. Appl. Phys. **82**, 3808 (1997).
[14]X. Tang, J. Katcki, E. Dubois, N. Reckinger, J. Ratajczak, G. Larrieu, P. Loumaye, O. Nisole, and V. Bayot, Solid-State Electron. **47**, 2105 (2003).
[15]Y.-L. Jiang, Q. Xie, C. Detavernier, R. L. Van Meirhaeghe, G.-P. Ru, X.-P. Qu, B.-Z. Li, A. Huang, and P. K. Chu, J. Vac. Sci. Technol. A **25**, 285 (2007).
[16]W. Huang, G. P. Ru, Y. L. Jiang, X. P. Qu, B. Z. Li, and R. Liu, Thin Solid Films **516**, 4252 (2008).
[17]F. P. Netzer and J. A. D. Matthew, Rep. Prog. Phys. **49**, 621 (1986).
[18]R. D. Thompson, K. N. Tu, and G. Ottaviani, J. Appl. Phys. **58**, 705 (1985).
[19]S. L. Liew, B. Balakrisnan, S. Y. Chow, M. Y. Lai, W. D. Wang, K. Y. Lee, C. S. Ho, T. Osipowicz, and D. Z. Chi, Thin Solid Films **504**, 81 (2006).

[20]Q. F. Daphne Yiew, Y. Setiawan, P. S. Lee, and D. Z. Chi, Thin Solid Films **504**, 91 (2006).
[21]E. Dubois and G. Larrieu, J. Appl. Phys. **96**, 729 (2004).
[22]E. J. Tan, M. L. Kon, K. L. Pey, P. S. Lee, Y. W. Zhang, W. D. Wang, and D. Z. Chi, Thin Solid Films **504**, 157 (2006).
[23]J. E. Baglin, F. M. d'Heurle, and C. S. Petersson, J. Appl. Phys. **52**, 2841 (1981).
[24]L. J. Chen, W. Lur, J. F. Chen, T. L. Lee, and J. M. Liang, *Rapid thermal and integrated processing III*, MRS Symposia Proceedings No. 342 (Materials Research Society, Pittsburgh, 1994), p. 99.
[25]L. J. Chen, Mater. Sci. Eng. R. **29**, 115 (2000).
[26]L. Osiceanu, Appl. Surf. Sci. **253**, 381 (2006).
[27]C. G. H. Walker, S. A. Morton, N. M. D. Brown, and J. A. D. Matthew, J. Electron Spectrosc. Relat. Phenom. **95**, 211 (1998).
[28]V. V. Atuchin, V. G. Kesler, N. V. Pervukhina, and Z. Zhang, J. Electron Spectrosc. Relat. Phenom. **152**, 18 (2006).
[29]S. Kennou, S. Ladas, M. G. Grimaldi, T. A. Nguyen Tan, and J. Y. Veuillen, Appl. Surf. Sci. **102**, 142 (1996).
[30]W. Huang, G. P. Ru, Y. L. Jiang, X. P. Qu, B. Z. Li, R. Liu, and F. Lu, J. Vac. Sci. Technol. B **26**, 164 (2008).
[31]M. Jun, M. Jang, Y. Kim, C. Choi, T. Kim, S. Oh, and S. Lee, J. Vac. Sci. Technol. B **26**, 137 (2008).
[32]C. S. Wu, D. M. Scott, and S. S. Lau, J. Appl. Phys. **58**, 1330 (1985).
[33]S. Vandré, T. Kalka, C. Preinesberger, and M. Dähne-Prietsch, Phys. Rev. Lett. **82**, 1927 (1999).